Nitrosomonas europaea Cytochrome P460 Is a Direct Link between Nitrification and Nitrous Oxide Emission

Jonathan D. Caranto, Avery C. Vilbert, and Kyle M. Lancaster *

Department of Chemistry and Chemical Biology, Baker Laboratory, Cornell University, Ithaca, NY 14853

SUPPORTING INFORMATION APPENDIX

Materials and Methods

General Considerations. Milli-Q water (18.2 MΩ; Millipore) was used in the preparation of all buffers and solutions. Disodium 1-(Hydroxyl-NNO-azoxy)-L-proline (PROLI-NONOate), and disodium diazen-1-ium-1,2,2 triolate ($Na_2N_2O_3$, Angeli's salt) were purchased from Cayman Chemicals. Hydroxylamine hydrochloride (NH_2OH•HCl) was purchased from Sigma Aldrich. All other chemicals were purchased from VWR International and used as obtained. A stock solution of PROLI-NONOate was prepared by dissolving 10 mg of PROLI-NONOate in 0.01 M NaOH. The concentration was measured spectrophotometrically (ε_{252nm} = 8400 M^{-1} cm^{-1}). Nitric oxide (NO) release from PROLI-NONOate was quantified by using $Na_2[Fe^{II}(EDTA)]$ to form Fe(EDTA)–NO complex ($\varepsilon_{440\ nm}$ = 900 M^{-1} cm^{-1}; EDTA = ethylenediaminetetraacetic acid) (1). Stock solutions of $Na_2N_2O_3$ were prepared by dissolving 40 mM $Na_2N_2O_3$in 0.01 M NaOH. The exact concentration of $Na_2N_2O_3$ was measured spectrophotometrically (ε_{237nm} = 6100 M^{-1} cm^{-1}) (2). Buffers were deoxygenated by bubbling with N_2 for at least 30 min. All reactions were prepared in an anaerobic chamber (Coy) with deoxygenated buffers unless otherwise noted. UV-visible (UV-vis) absorption spectra measurements were performed with a Cary 60 UV-vis spectrometer. Data were fit using Igor Pro version 6.37 (WaveMetrics).

Protein Expression and Purification. A gene encoding *Nitrosomonas europaea* cytochrome (cyt) P460 was codon-optimized for *Escherichia coli* (*E. coli)*, synthesized, and cloned into the pET22b (+) vector by GenScript, Inc. Cyt P460 was expressed and purified as described by Elmore (3) with slight modification. The expression plasmid and pEC86 containing the cyt *c* maturation genes ccmABCDEFGH (4) (provided by H. B. Gray) were co-transformed into *E. coli* strain BL21(DE3) with selection on lysogeny broth plates supplemented with 100 μg mL^{-1} each ampicillin and chloramphenicol. A single colony each was used to inoculate two 3 mL lysogeny broth starter cultures containing 100 μg mL^{-1} ampicillin and chloramphenicol. These starter cultures were incubated with shaking at 37 °C for 6 h and used to inoculate two 6 L culture flasks containing 2.5 L Terrific Broth medium and 0.5% glycerol (0.1% inoculum). The cultures were grown at 30 °C until the optical density at 600 nm reached 0.7, at which point expression was induced by adding isopropyl β-D-1-thiogalactopyranoside to a final concentration of 0.4 mM. The cells were harvested via centrifugation 6 to 8 h post-induction to yield a green cell pellet. The cells were then lysed with sonication in 20 mM Tris (pH 8.0) containing 150 mM NaCl and 0.01% Triton X. The green lysate was clarified via centrifugation for 45 min at 35,000 × *g* relative centrifugal force. The supernatant was applied to a HisTrap HP Ni affinity column (GE Lifesciences), washed with 20 mM Tris (pH 8.0) containing 150 mM NaCl, and eluted with 20 mM Tris (pH 8.0) containing 150 mM NaCl and 330 mM imidazole. The fractions containing cyt P460 were combined, concentrated and purified to homogeneity using a HiLoad Superdex 75 size-exclusion column equilibrated with a running buffer of 50 mM morpholinepropanesulfonic acid (pH 7.2) containing 150 mM NaCl. Protein purity was evaluated with sodium dodecyl sulfate polyacrylamide gel electrophoresis. Typical purifications yielded Reinheitszahl values (R_z, or the purity ratio of $A_{440\ nm}/A_{280\ nm}$) of ca. 1.5.

Steady-State Activity Assays. All assays were performed in septum-sealed cuvettes flushed with N_2 gas. NH_2OH • HCl (69 mg; 1 mmol) was equilibrated in an anaerobic environment overnight and then dissolved in 1 mL of deoxygenated water to yield a 1 M solution. This solution was serially diluted 20,000-fold in deoxygenated water and assayed by the method of Frear and Burrell (5) for accurate determination of the stock NH_2OH concentration. Final concentrations of 50 μM 2,6-dichlorophenolindophenol (DCPIP), 6 μM phenazine methosulfate (PMS), and 1 μM cyt P460 were added to 2 mL of deoxygenated 50 mM sodium phosphate (pH 8.0). The reaction was initiated by adding an appropriate volume of the NH_2OH stock solution to the reaction mixture through the septum with a Hamilton syringe. The reaction progress was followed by

monitoring the absorption of DCPIP at 605 nm. The rate of the first 10% of the total oxidant consumption was determined through linear regression. This rate was converted to the rate of oxidant consumed by using $\varepsilon_{605\ nm} = 20.6\ mM^{-1}cm^{-1}$ (6). At least three trials for each NH_2OH concentration were averaged and the standard deviations plotted. The initial rates were plotted versus NH_2OH concentration, and the resulting plot was fit using linear regression.

Pseudo First-Order Kinetics Measurements. Stock solutions of $[Ru(NH_3)_6]Cl_3$ were prepared by equilibrating 62 mg of $[Ru(NH_3)_6]Cl_3$ in the anaerobic chamber overnight. $[Ru(NH_3)_6]Cl_3$ was then dissolved in 1 mL of deoxygenated water to generate a 200 mM solution. The dependence of NH_2OH on the reaction was measured by monitoring the absorbance of the 455 nm intermediate. Cyt P460 (10 μM) and $[Ru(NH_3)_6]Cl_3$ (50 μM) were combined with 2 mL of 50 mM 4-(2-hydroxyethyl)-1-piperazine-ethanesulphonic acid (HEPES) buffer (pH 8.0) in an anaerobic cuvette. The reaction was initiated by using a Hamilton syringe to add the appropriate volume of NH_2OH • HCl to the reaction mixture through the septum on the cuvette. Measurements were carried out from 0.2 mM to 10 mM NH_2OH. The formation and decay of the 455 nm intermediate were monitored with full-wavelength kinetic UV-vis absorption scans at intervals of 0.5 min for 0 to 10 min, 1 min from 10 to 20 min, and 2 min from 20 to 40 min. The sum of two exponentials (Equation S1) were fit to the kinetic traces.

$$A_0 + \sum_i^n A_i e^{-k_{obs(i)}t} \qquad \text{(Equation S1)}$$

The fits provided observed rate constants (k_{obs}) for each NH_2OH concentration ($k_{obs} = k[NH_2OH]$). The plot of the slower of the two k_{obs} versus NH_2OH concentration was fit to a linear equation.

Generation of $\{FeNO\}^6$. Cyt P460 (10 μM) was combined with 2 mL of 200 mM HEPES buffer (pH 8.0) in an anaerobic cuvette. The $\{FeNO\}^6$ species was generated using a Hamilton syringe and adding 5 μM aliquots of PROLI-NONOATE to the cuvette until a 1 mol equivalent of the 455 nm species was reached. The titration was monitored with UV-vis spectroscopy. The reaction between the 455 nm "shunted" $\{FeNO\}^6$ species and NH_2OH was initiated by using a Hamilton syringe and adding 2 mM NH_2OH to the cuvette containing the $\{FeNO\}^6$ species. Full-wavelength UV-vis kinetic traces were measured at intervals of 0.5 min for 10 min, 1 min for 20 min, and 2 min for 40 min.

Pseudo first order kinetic data for reaction of shunted $\{FeNO\}^6$ with NH_2OH: The $\{FeNO\}^6$ species was prepared as stated above. Cyt P460 (30μM) and 1 equiv. of PROLI-NONOATE (60μM NO) were combined with 2mL of 200mM HEPES buffer (pH 8.0) in a septum-sealed cuvette. The reaction between the shunted $\{FeNO\}^6$ and NH_2OH was initiated by using a Hamilton syringe and adding the appropriate volume of NH_2OH•HCl to the cuvette. Measurements were carried out between 2 mM and 8 mM NH_2OH. The dependence of NH_2OH on the shunted $\{FeNO\}^6$ was measured by monitoring the absorbance at 455nm. The decay of the $\{FeNO\}^6$ species was monitored with full-wavelength kinetic UV/vis absorption scans at intervals of 0.5 min for 10min, 1 min for 20 min and 2 min for 40 min. Single exponential functions (equation S1, $n = 1$) were fit to the data. Observed rate constants (k_{obs}) from the provided fits for each concentration of NH_2OH ($k_{obs} = k[NH_2OH]$) were then plotted against NH_2OH concentration. The k_{obs} versus NH_2OH concentration plot was then fit using linear regression in IGOR Pro 6.37.

Generation of the $\{FeNO\}^7$. Cyt P460 (10 μM) was combined with 2 mL of 200 mM HEPES buffer (pH 8.0) in an anaerobic cuvette. Cyt P460 (10μM) was incubated with 50 μM $Na_2N_2O_3$ to generate the $\{FeNO\}^7$ species. $[Ru(NH_3)_6]Cl_3$ (100 μM) was added to the $\{FeNO\}^7$ and monitored

by UV-vis (200 to 800 nm) at intervals of 0.5 min for 10 min and 1 min for 20 min. The reactivity of $\{FeNO\}^7$ with NH_2OH was also measured. The $\{FeNO\}^7$ species was generated as described above, and the reaction was initiated with 10 mM NH_2OH. The reaction was monitored by UV-vis (200 to 800 nm) at intervals of 0.5 min for 10 min and 1 min for 20 min.

Measurement of N_2O. All reactions were prepared and sealed in 5 mL headspace gas chromatography (GC) vials (Wheaton). The concentration of formed N_2O was analyzed with GC (Agilent) or GC–mass spectroscopy (GC–MS; JEOL GC-MATE II), or an N_2O microsensor housed within a septum-piercing needle (Unisense). The N_2O concentration was measured in the headspace of solutions containing cyt P460 (5 μM), PMS (1 mM), and various amounts of NH_2OH. The headspace was measured with GC analysis using a Supel-Q PLOT column (30 mm × 0.32 mm). The concentration of N_2O formed during the $\{FeNO\}^6$ shunted experiments was measured with GC-MS using an RT Q bond column. GC-MS samples (500 μL) were prepared in a Coy chamber with 1.5 mL headspace vials (Agilent). The $\{FeNO\}^6$ was generated by incubating cyt P460 (5 μM) and various amounts of PROLI-NONOATE. The reaction was initiated by adding 10 mM $^{14}NH_2OH$ or $^{15}NH_2OH$ and was allowed to react in the Coy chamber for 2 h. After 2 h, the reaction was quenched with 1 M phosphoric acid.

Electron Paramagnetic Resonance (EPR). The protein concentration used was 0.3 mM in 200 mM HEPES (pH 8.0) with 25% (v/v) glycerol. The EPR spectra were recorded at X-band (9.40 GHz) on a Bruker Elexsys-II spectrometer equipped with a liquid He cryostat maintained at 10 or 20 K. EPR data were simulated, and spin concentrations were determined by using SpinCount (7).

Measurement of k_{obs} for oxidation of Fe^{II} cyt P460 by stopped-flow spectrophotometry. As isolated cyt P460 was treated with 0.5 equivalents of $Na_2S_2O_4$ (dithionite) to produce Fe^{II} cyt P460. The stopped-flow experiments were performed using a Bio-Logic SFM-300 with light monochromated to 463 nm and monitored using a photomultiplier tube (Bio-Logic Science Instruments SAS). O_2 in the mixing circuit was scavenged by treatment with 10 mM $Na_2S_2O_4$ for one hour. Excess $Na_2S_2O_4$ was then washed out with 4x5 ml of degassed 50 mM sodium phosphate, pH 8.0 or degassed water. 90 μM of Fe^{II} cyt P460 in 50 mM sodium phosphate, pH 8.0 was anaerobically loaded into the stopped-flow mixing circuit and mixed 1:1 (v/v) with either 2 mM $[Ru(NH_3)_6]Cl_3$ or 4 mM NH_2OH in degassed water. The Fe^{II} cyt P460 vs. 1 mM NO was performed as a sequential mixing experiment where a 4 mM stock solution of PROLI-NONOate was pre-mixed 1:1 (v/v) with 250 mM sodium phosphate, pH 8.0 and allowed to decay in the delay line for 30 seconds. The resulting 2 mM NO solution was then mixed 1:1 (v/v) against 90 μM of Fe^{II} cyt P460 in second mixing step. For all experiments, the consumption of Fe^{II} cyt P460 was monitored by the loss of the 463-nm absorption band corresponding to the Soret peak of Fe^{II} cyt P460. All experiments were performed at 25 ºC.

Supplementary Figures

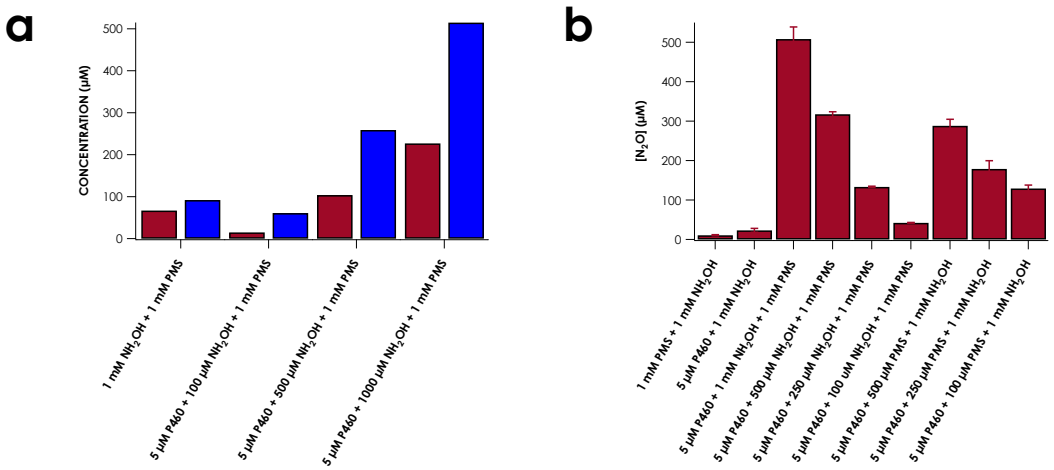

Fig. S1. N_2O and NO_2^- production by cytochrome (cyt) P460 under either (a) aerobic or (b) anaerobic conditions and with varying NH_2OH and oxidant concentrations. NO_2^- concentration (blue bars) was measured by UV/vis absorption spectrometry after treatment of the sample with Griess reagent. N_2O concentration (red bars) was monitored with gas chromatography. No blue bars are shown for the anaerobic experiments as NO_2^- was never detected under these conditions. Data points in (b) are averages of triplicate reactions of 5 µM cyt P460 in anaerobic 50 mM 4-(2-hydroxyethyl)-1-piperazine-ethanesulphonic acid (HEPES), pH 8.0, at 25 ^oC overnight. Error bars in (b) represent one standard deviation of three trials.

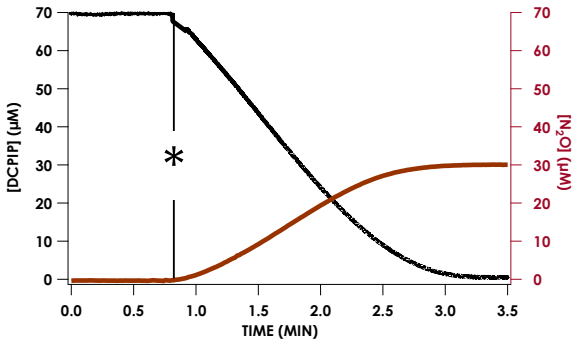

Fig. S2. Representative time courses of 2,6-dichlorophenolindophenol (DCPIP) consumption (black trace) and N_2O production (red trace) during the reaction of 1 µM cyt P460 with 5 mM NH_2OH and 70 µM DCPIP in anaerobic 50 mM phosphate, pH 8.0, at 25 °C. The reaction was initiated by the addition of 5mM NH_2OH at the time point indicated by (*). Consumption of DCPIP was monitored by its absorbance at 605 nm. N_2O production was measured with an N_2O-selective electrode. Initial rates were measured through fitting to a linear equation. Initial rates showed a DCPIP consumption rate of 40 µM min^{-1} and an N_2O production rate of 20 µM min^{-1}.

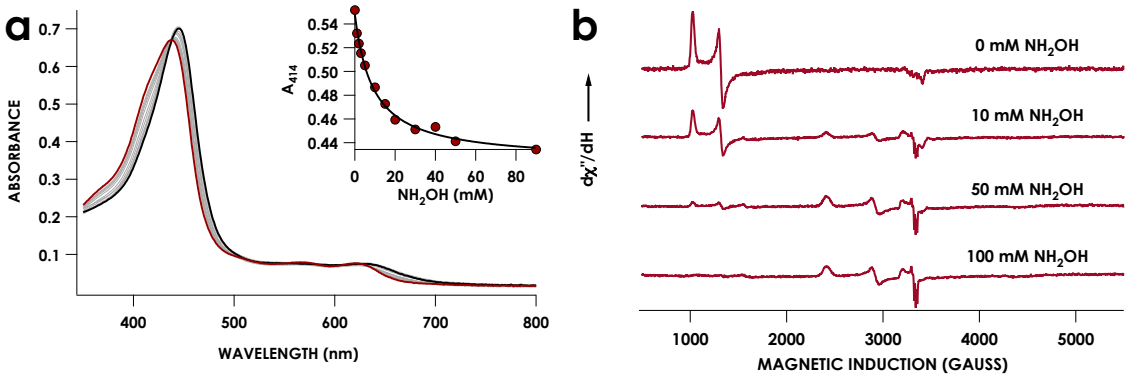

Fig. S3. Cyt P460 and NH_2OH titration curve as monitored by (a) UV/visible (UV/vis) absorption and (b) electron paramagnetic resonance (EPR) spectroscopy. (a) UV-vis traces of 12 µM cyt P460 titrated with various amounts of NH_2OH in anaerobic 50 mM sodium phosphate, pH 8.0, at 25 °C. Inset shows a plot of $A_{414\ nm}$ versus NH_2OH concentration with a fit generated using the following hyperbolic equation: $A_{414\ nm} = \frac{\Delta A_{414\ nm}[NH_2OH]_0}{K_d + [NH_2OH]_0}$. (b) EPR spectra of 170 µM cyt P460 mixed with 0, 10, 50, or 100 mM NH_2OH in anaerobic 50 mM sodium phosphate, pH 8.0. The spectra were collected at 10 K and a microwave power of 6 µW. Table ST1 shows the concentration of each EPR signal as determined through simulation.

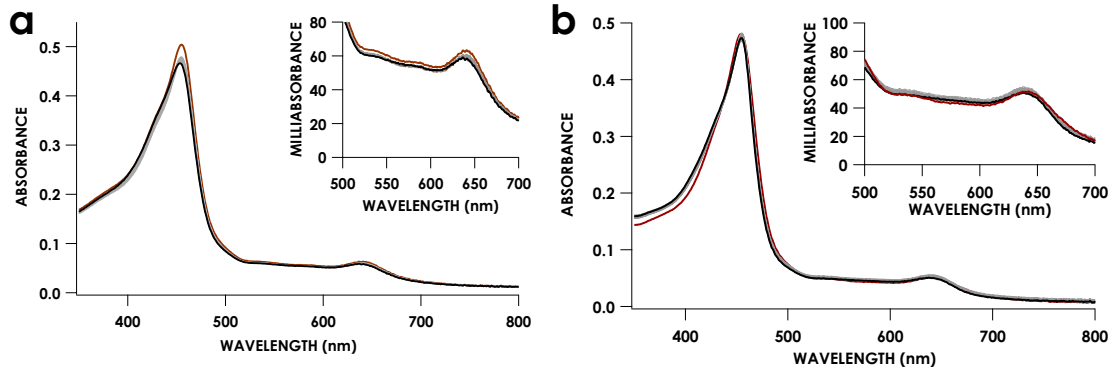

Fig. S4. UV/vis absorption spectrum of 10 µM cyt P460 incubated with 50 µM $Na_2N_2O_3$ for 30 min and then reacted with either (a) NH_2OH or (b) $[Ru(NH3)_6]Cl_3$. All reactions were performed in anaerobic 200 mM HEPES, pH 8.0, at 25 °C.

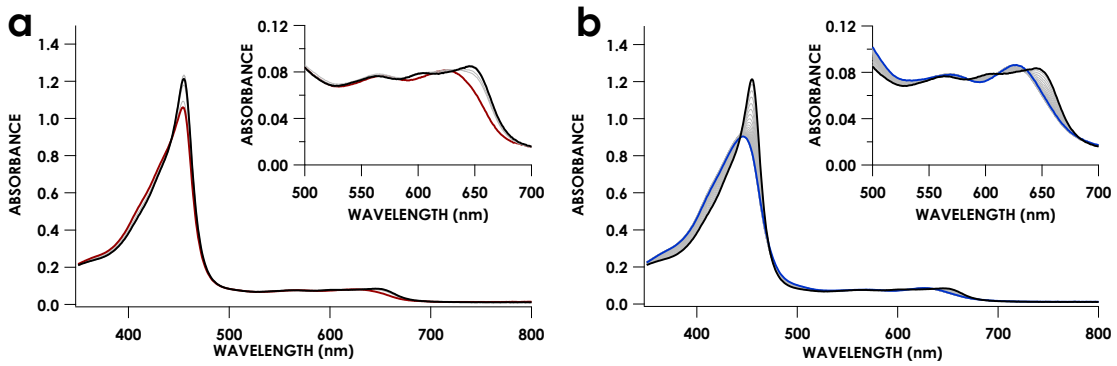

Figure S5. Representative UV/vis absorption spectral time courses of the (a) accumulation and (b) decay of the 455 nm intermediate during the reaction of 10 µM cyt P460, 200 µM $[Ru(NH_3)_6]Cl_3$, and 6 mM NH_2OH in anaerobic 50 mM HEPES, pH 8.0, at 25 °C. The reaction was initiated by the addition of $[Ru(NH_3)_6]Cl_3$. The red trace in (a) is the UV/vis spectrum collected immediately after the addition of NH_2OH, and the black trace is the accumulated 455 nm intermediate. The blue trace in (b) is the spectrum of the decay product. The insets in both figures highlight the Q-band region.

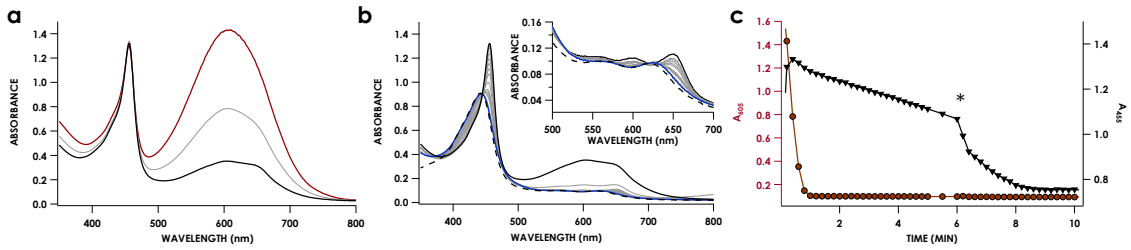

Figure S6. Representative spectral time courses of the (a) accumulation and (b) decay of the 455 nm intermediate during the reaction of 12 µM cyt P460 with 1 mM NH_2OH and 70 µM DCPIP in anaerobic 50 mM sodium phosphate, pH 8.0, at 25 °C . The reaction was initiated by the addition of 1 mM NH_2OH. (b) Representative spectral time course of the decay of the 455 nm intermediate before and after adding another 10 mM NH_2OH. In kinetic traces of the decay of the 455 nm intermediate, black is the accumulated intermediate and blue is the final decay product. The inset highlights the Q-band region. The dashed spectrum shows the product of incubating cyt P460 with 10 mM NH_2OH. (c) Representative 455 and 605 nm traces following the accumulation and decay of the 455 nm intermediate (red trace) and the consumption of DCPIP (black trace). The asterisk indicates the addition of 10 mM NH_2OH to the 455 nm intermediate once the DCPIP has been consumed.

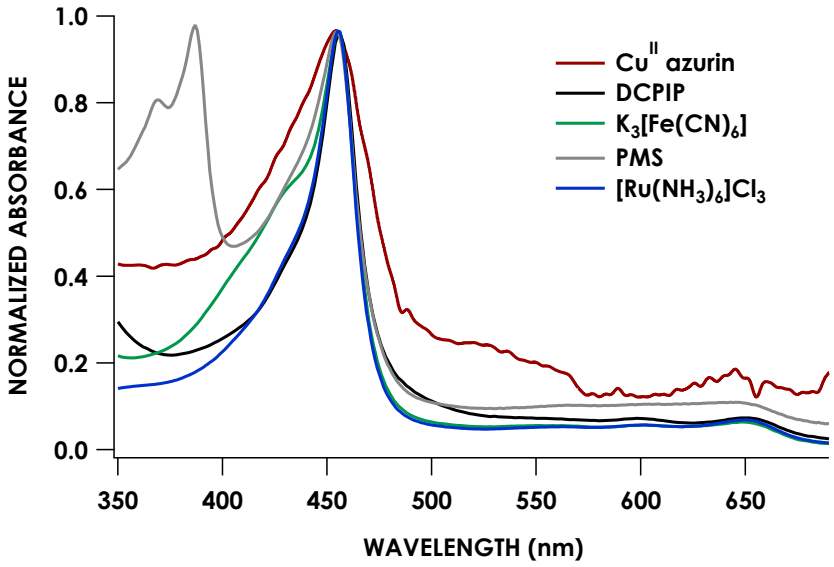

Fig. S7. UV/vis absorption spectra of 455 nm intermediate prepared with various oxidants.

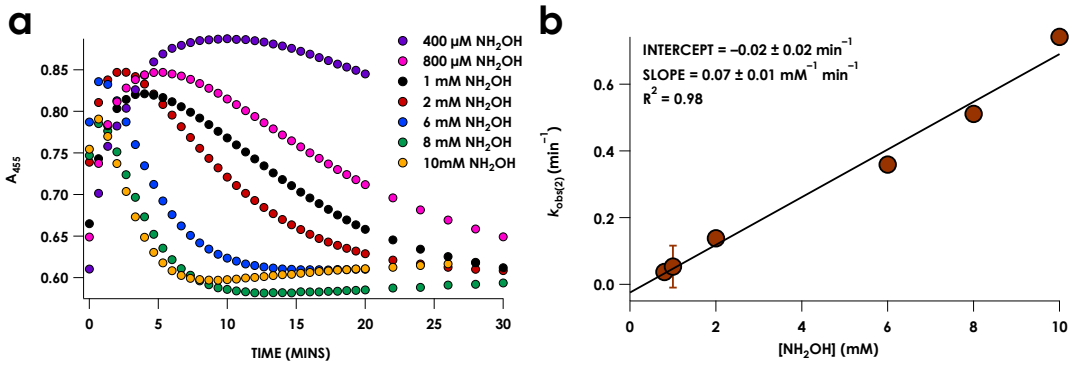

Fig. S8. (a) Representative $A_{455\ nm}$ traces monitoring the reaction of cyt P460 (10 µM), and $[Ru(NH_3)_6]Cl_3$ (100 µM) with varying NH_2OH concentrations. (b) Plot of k_{obs2} determined by fitting Equation S1 to traces in panel a versus NH_2OH concentration.

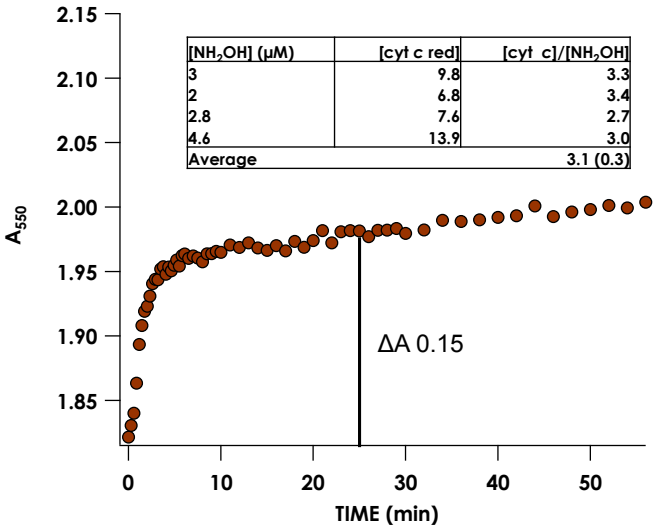

Figure S9. A 550 nm trace monitoring the reduction of cyt *c* in the presence of NH_2OH at sub-stoichiometric concentrations relative to cyt P460. Final reaction conditions: 15 μM cyt P460, 23 μM cyt *c* in anaerobic sodium phosphate, pH 8.0 at 25 °C. The reaction was initiated by adding 2.8 μM NH_2OH.

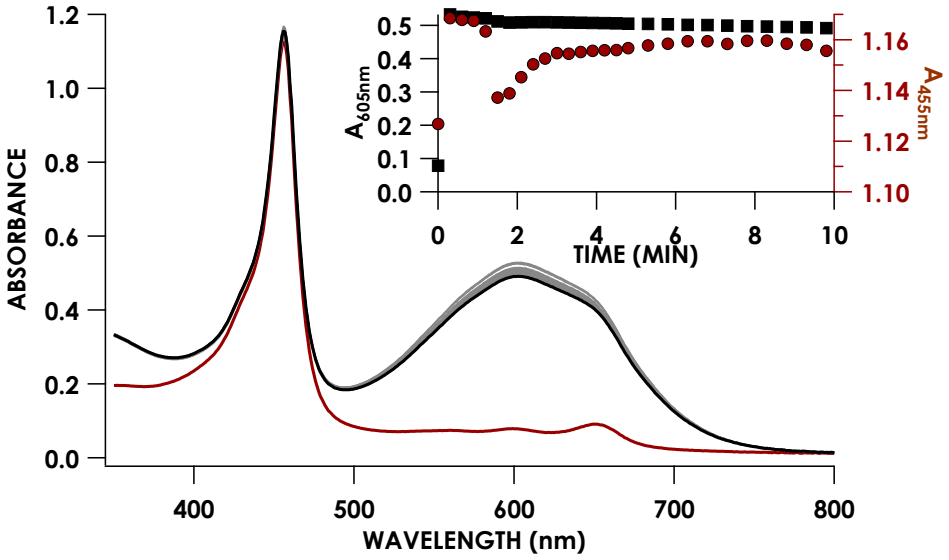

Fig. S10. UV-vis spectrum demonstrating the stability of $\{FeNO\}^6$ with DCPIP. Treatment of cyt P460 (16 μM) and 1 equiv. of NO generates the $\{FeNO\}^6$ species (red trace). 30 μM DCPIP is subsequently added. The inset single-wavelength traces follow the absorbance at 605 nm for DCPIP (black squares) and the absorbance of the 455 nm intermediate (red circles).

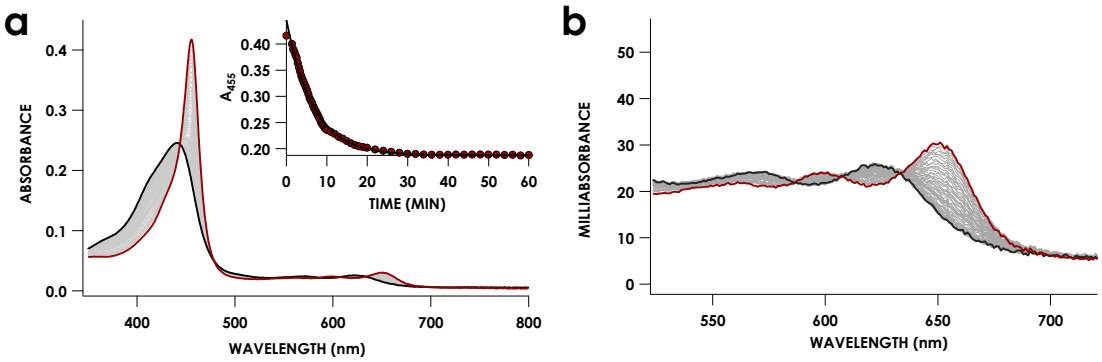

Fig. S11. Reaction of $\{FeNO\}^6$ formed via the NO shunt with NH_2OH. The $\{FeNO\}^6$ species was generated with 5 µM cyt P460 and 16 µM PROLI-NONOate in anaerobic 200 mM HEPES, pH 8.0. The decay of $\{FeNO\}^6$ was initiated by addition of a final concentration of 2 mM NH_2OH and followed by observing the decay of the 455 nm Soret peak. (a) UV/vis absorption spectral time course of decay of the 455 nm (red) Soret peak to the Fe^{III}–NH_2OH adduct (black). Inset shows the $A_{455\ nm}$ trace. (b) Expansion of the Q-band region. Experiments were performed at 25 °C at pH 8.0.

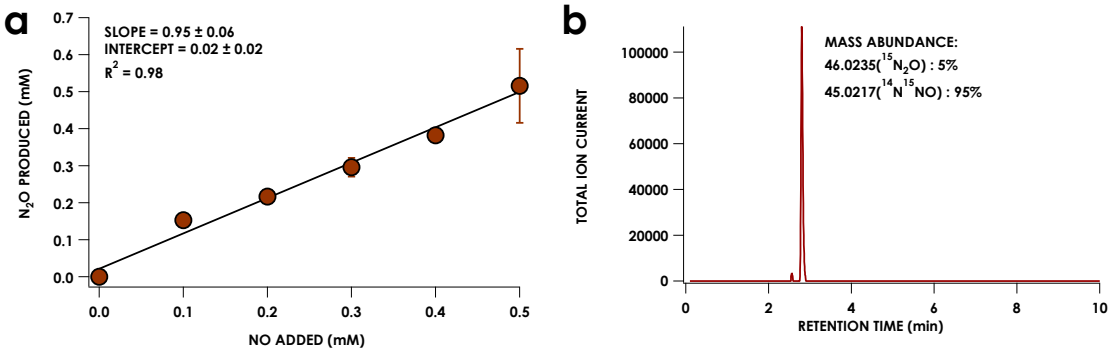

Fig. S12. Gas chromatography mass spectroscopy (GC-MS) analysis of $\{FeNO\}^6$ shunt experiments with the addition of 10 mM NH_2OH. The $\{FeNO\}^6$ was generated by mixing 5 µM cyt P460 with varying amounts of PROLI-NONOate. The reaction was initiated by the addition of 10 mM NH_2OH. (a) Stoichiometry results of the GC-MS analysis showing a 1:1 ratio of added NO to produced N_2O. (b) MS chromatogram showing that the reaction of $^{15}NH_2OH$ with $\{FeNO\}^6$ P460 generated using ^{14}NO produces only mixed-isotope N_2O.

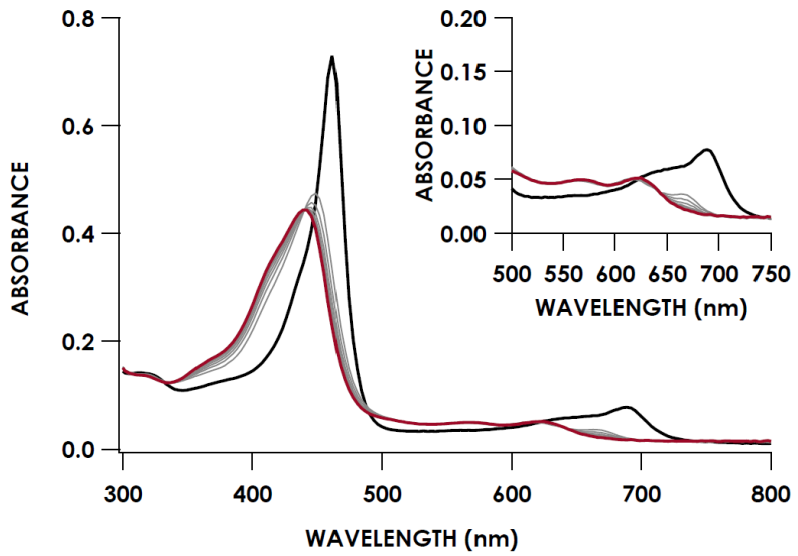

Fig. S13. UV/vis absorption spectral time course of 30 µM Fe^{II} cyt P460 mixed with 10 mM NH_2OH in anaerobic 50 mM sodium phosphate, pH 8.0 at 25 °C. The black spectrum is the spectrum of the Fe^{II} cyt P460 before adding NH_2OH. Grey traces are collect every 0.3 seconds after NH_2OH addition. The red spectrum is the final spectrum at 3.0 seconds.

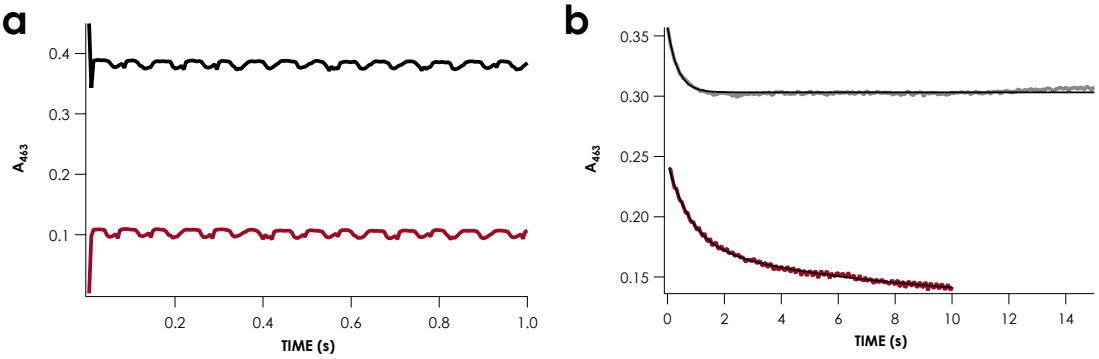

Fig. S14. Single-wavelength (463 nm) stopped-flow time courses of Fe^{II} cyt P460 (a) before (black trace) and after (red trace) mixing with 1 mM $[Ru(NH_3)_6]Cl_3$ and (b) after mixing with 1 mM NO (gray trace) or 2 mM NH_2OH (red trace). Fits to the data are shown in black. Conditions after mixing were 7 µM cyt P460 in anaerobic 50 mM sodium phosphate, pH 8.0 at 25 °C.

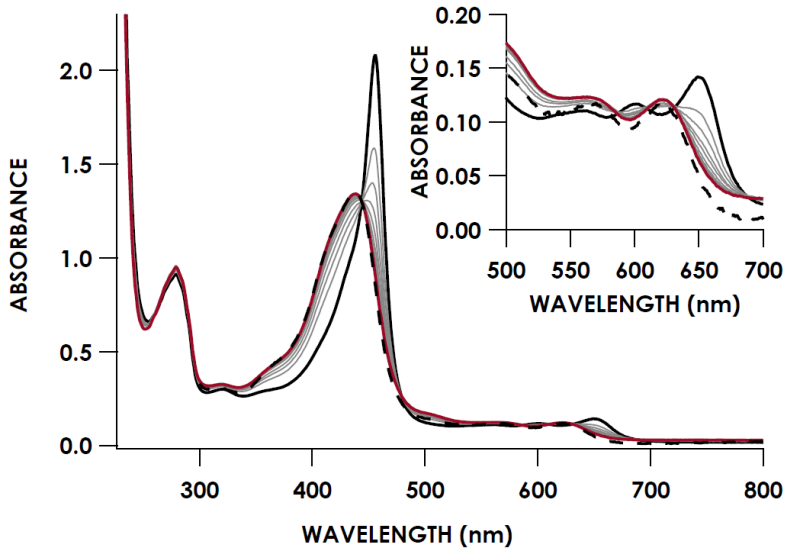

Fig. S15. 24-min UV/vis absorption spectral time course of 30 µM as-isolated cyt P460 mixed with 1 equiv. NO that has been exposed to air in 50 mM sodium phosphate, pH 8.0 at 25 ^{o}C. Inset shows expanded Q-band region. Solid black trace is the spectrum of the {FeNO}^{6} generated from addition of 0.5 equivalents of PROLI-NONOate to the as isolated cyt P460. Grey traces are collected in 2 minute increments after exposure of the sample to air. Red trace is the final spectrum at 24 minutes. Dashed black trace is the spectrum of 30 µM as isolated cyt P460 for comparison.

Supplementary Tables

Table ST1. N_2O production by cyt P460 at varying concentrations of NH_2OH or PMS[a]

[NH_2OH] (µM)[b]	[N_2O] (µM)
0	23
100	42
250	134
500	318
1000	509
[PMS] (µM)[c]	**[N_2O] (µM)**
0	23
100	129
250	179
500	288
1000	509
	[N_2O] (µM)
1 mM PMS + 1 mM NH_2OH	11

[a]Reaction conditions were 5 µM cyt P460 in anaerobic 50 mM sodium phosphate, pH 8.0 at 37 °C
[b][NH_2OH] varied with constant [PMS] of 1 mM.
[c][PMS] varied with constant [NH_2OH] of 1 mM

Table ST2. Oxidation of NH_2OH by cyt P460 under aerobic conditions.[a]

$[NH_2OH]_0$ (μM)	$[N_2O]$ (μM)	$[NO_2^-]$ (μM)	Total NH_2OH consumed (μM)	% NH_2OH converted to N_2O	% NH_2OH converted to NO_2^-
100	15	61	91	33	67
500	104	259	467	45	55
1000	227	515	969	47	53

[a]Reaction conditions were 5 μM cyt P460, 1 mM PMS in 50 mM sodium phosphate, pH 8.0 at 37 °C

Table ST3. Concentrations of spins observed in Figure S3(b).[a]

$[NH_2OH]$ (mM)	S = 5/2 (μM) (Fe^{III}–OH_2)	S = 1/2 (μM) (Fe^{III}–NH_2OH)	{FeNO}7 (μM)
0	171 (100)	0 (0)	0 (0)
10	82 (50)	73 (45)	8 (5)
50	13 (8)	150 (87)	8 (5)
100	0 (0)	160 (95)	8 (5)

[a]Parenthetical values indicate the percentage of total Fe in each sample comprised by these species.

Table ST4. Spin Hamiltonian parameters from SpinCount (7) simulations of EPR spectra in Fig. 5.

Species	g_1 (σg_1)	g_2 (σg_2)	g_3 (σg_3)	^{14}N A_1 (MHz)	^{14}N A_2 (MHz)	^{14}N A_3 (MHz)	E/D
Fe^{III}–OH_2	1.92	1.96	2	—	—	—	0.03
Fe^{III}–NH_2OH	1.52 (0.06)	2.29 (0.03)	2.78 (0.05)	—	—	—	—
{FeNO}^{7}	2.012 (0.0002)	2.026 (0.003)	2.098 (0.0002)	50	57	45	—

References

1. Hayashi T, Caranto JD, Wampler DA, Kurtz Jr DM, Moënne-Loccoz P (2010) Insights into the nitric oxide reductase mechanism of flavodiiron proteins from a flavin-free enzyme. *Biochemistry* 49(33):7040-7049.
2. Peyrot F, Fernandez BO, Bryan NS, Feelisch M, & Ducrocq C (2006) *N*-Nitroso products from the reaction of indoles with Angeli's salt. *Chem Res Toxicol* 19(1):58-67.
3. Elmore BO, Pearson AR, Wilmot CM, Hooper AB (2006) Expression, purification, crystallization and preliminary X-ray diffraction of a novel *Nitrosomonas europaea* cytochrome, cytochrome P460. *Acta Crystallogr F* 62(4):395-398.
4. Thöny-Meyer L, Fischer F, Künzler P, Ritz D, Hennecke H (1995) *Escherichia coli* genes required for cytochrome c maturation. *J Bacteriol* 177(15):4321-4326.
5. Frear D & Burrell R (1955) Spectrophotometric method for determining hydroxylamine reductase activity in higher plants. *Anal Chem* 27(10):1664-1665.
6. Williamson G & Engel PC (1984) Butyryl-CoA dehydrogenase from *Megasphaera elsdenii*. Specificity of the catalytic reaction. *Biochem J* 218(2):521-529.
7. Golombek AP & Hendrich MP (2003) Quantitative analysis of dinuclear manganese (II) EPR spectra. *J Magn Reson* 165(1):33-48.